Ground- and Excited-State Double Proton Transfer in Lumichrome/Acetic Acid System: Theoretical and Experimental Approach

Ewa Sikorska,[†] Igor Khmelinskii,[‡] Marcin Hoffmann,[§,⊥] Isabel F. Machado,[||] Luis F. V. Ferreira,[||] Krzysztof Dobek,[#] Jerzy Karolczak,[#,○] Alina Krawczyk,[§] Małgorzata Insińska-Rak,[§] and Marek Sikorski*[,§]

Faculty of Commodity Science, Poznań University of Economics, al. Niepodległości 10, 60-967 Poznań, Poland, Universidade do Algarve, DQB, FCT, Campus de Gambelas, Faro 8005-139, Portugal, Faculty of Chemistry, A. Mickiewicz University, Grunwaldzka 6, 60-780 Poznań, Poland, BioInfoBank Institute, Limanowskiego 24A, 60-744 Poznań, Poland, Centro de Química-Física Molecular, Complexo Interdisciplinar, Instituto Superior Técnico, 1049-001 Lisbon, Portugal, Faculty of Physics, A. Mickiewicz University, Umultowska 85, 61-614 Poznań, Poland, and Center for Ultrafast Laser Spectroscopy, A. Mickiewicz University, Umultowska 85, 61-614 Poznań, Poland

Received: July 18, 2005; In Final Form: October 31, 2005

Experimental time-resolved spectral and photon counting kinetic results confirm formation of an isoalloxazinic excited state via excited-state double proton transfer (ESDPT) catalyzed by a carboxylic acid molecule that forms a hydrogen-bond complex with the parent alloxazine molecule. This isoalloxazinic tautomer manifests itself as a distinct long-lived emissive species formed only in such alloxazine derivatives that were not substituted at the N(1) nitrogen atom, being a product of the excited-state reaction occurring from the alloxazinic excited state. Theoretical calculations support the idea that the ESDPT occurs by the concerted mechanism. The calculated activation barrier in the excited state is much lower than the same barrier in the ground state and even disappears for the HOMO-1 to LUMO excitation, which explains the fact that the reaction takes place in the excited-state only. The reaction rate estimated from the emission kinetics is ca. 1.4×10^8 dm^3 mol^{-1} s^{-1} in ethanolic solutions of lumichrome with added acetic acid.

Introduction

One of the fundamental aspects of the excited state double proton transfer (ESDPT) is whether the reaction mechanism is concerted or stepwise. Since the first report in 1969 on the ESDPT discovery in 7-azaindole,[1] the ESDPT has been studied extensively. The well-known model of the ESDPT reaction in 7-azaindole assumes formation of a precursor, doubly hydrogen-bonded dimer of 7-azaindole. Despite intensive studies on 7-azaindole, the definite answer about the ESDPT mechanism remains an issue of continuing controversy both in experimental[2−7] and theoretical studies.[7−13]

The phenomenon of ESDPT is in no way limited to 7-azaindole dimers. In fact, it was shown that the ESDPT might occur not only in 7-azaindole but in other molecules in the presence of compounds having proton donor and acceptor functions that are able to form hydrogen bonds of appropriate strength and conformation to yield appropriate cyclic complexes, e.g., carboxylic acids, alcohols or water. For a review of the literature, see for example refs 14 and 15 and references therein. Some of the very recent developments on the evidence of complete localization in the lowest excited electronic state of asymmetric isotopomers,[16] cooperative nature of double-proton transfer revealed by H/D kinetic isotopic effects,[17] and on the reaction mechanism studied by picosecond time-resolved REMPI spectroscopy[18] and some other aspects[19−22] of ESDPT reaction can be found in a series of papers by Sekiya et al. Following the initial studies of 7-azaindole, a number of other systems including hydroxyquinolines, carbazoles, indoles, β-carbolines, and other molecules have been intensively examined, see for example[14] and references therein, among them lumichrome = 7,8-dimethylalloxazine = 7,8-dimethylbenzo[*g*]-pteridine-2,4(1*H*,3*H*)-dione (see Figure 1) the representative of alloxazines (benzo[*g*]pteridine-2,4(1*H*,3*H*)-diones).

The excited state proton transfer reaction in lumichrome had been one of the first systems studied. As early as in 1965, the existence of alloxazinic and isoalloxazinic emission in lumichrome and related compounds was first explained on the basis of solvent effect on emission involving possible proton-transfer reaction.[23,24] The very first mechanism for the excited-state proton transfer in lumichrome in the presence of acetic acid had been proposed by Kozioł, Koziołowa, Song, and coworkers.[25−27] This mechanism assumes formation of 1:1 eight-membered cyclic complexes between lumichrome and acetic acid with hydrogen bonds between acetic acid and lumichrome molecule at N(1)−H and N(10). The increase in the basicity of the N(10) nitrogen atom and an increase in the acidity of the N(1)−H group after excitation provide the driving force for the proton shift between these two nitrogen atoms. Kasha proposed an analogous mechanism, with six-membered complex between lumichrome and acetic acid.[28] Acetic acid is of special interest as it can form eight-membered cyclic hydrogen-bonded complexes with lumichrome. The use of acetic acid as a proton-

* Corresponding author. Fax: +48 61 8658008. Telephone: +48 61 8291309. E-Mail: sikorski@amu.edu.pl.
[†] Faculty of Commodity Science, Poznań University of Economics.
[‡] Universidade do Algarve, DQB, FCT.
[§] Faculty of Chemistry, A. Mickiewicz University.
[⊥] BioInfoBank Institute.
[||] Centro de Química-Física Molecular, Complexo Interdisciplinar, Instituto Superior Técnico.
[#] Faculty of Physics, A. Mickiewicz University.
[○] Center for Ultrafast Laser Spectroscopy, A. Mickiewicz University.

10.1021/jp053951d CCC: $30.25
Published on Web 12/06/2005

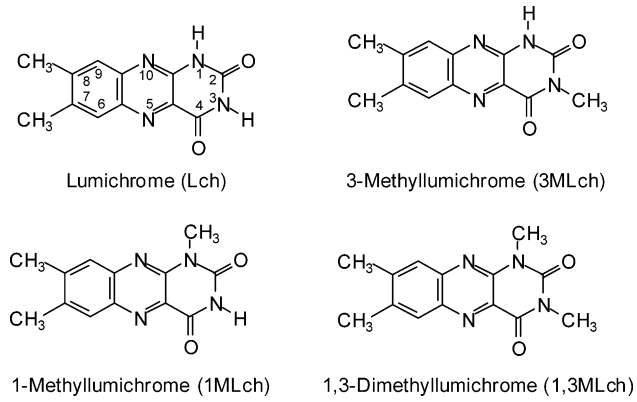

Figure 1. Structures of lumichrome, 1-methyllumichrome, 3-methyllumichrome, and 1,3-dimethyllumichrome.

transfer agent is particularly justified, as the molecular structure of the agent molecule (e.g., acetic acid in the acetic acid/lumichrome complex) remains unchanged upon performance of the ESDPT process. Therefore, acetic acid serves as a simple yet powerful catalyst for the ESDPT process.[29] Following the initial studies in the 1960s, considerable work has been done to study the mechanism of excited-state proton-transfer reaction in lumichrome−acetic acid and other complexes.[25,27,28,30−42] Despite the early discovery and the number of reported studies, there still remain several discrepancies in the results concerning the mechanism and kinetics of the ESDPT reaction in the alloxazines. One of the main controversies concerns the rates of the excited state process. Some results, based on time-resolved studies, have revealed a relatively high rate constant of the process discussed, of about 10^{12} s^{-1}.[43] On the other hand, Choi et al.[37] reported considerably lower rate constants of the excited-state proton transfer. However, Choi et al. have estimated the proton transfer rates from the steady state ratios of the normal and tautomeric emission, assuming a diffusion-controlled mechanism. The ongoing discussion about the mechanism is closely related to the controversies concerning the reaction rate constant. Our recent results in 1,2-dichloroethane, acetonitrile, and pure acetic acid (AA) show that the mechanism of acetic acid catalyzed tautomerism of lumichrome depends on the solvent.[31] We should underline a general lack of information on the excited-state proton-transfer reaction in alloxazines studied by theoretical methods. Recently, we have studied the acid−base properties of alloxazine and its methyl derivatives in their ground and first excited singlet states.[41] The concept of an effective electronic valence potential had been applied to predict the changes in basicity and acidity of heteroatoms upon excitation and substitution. A good linear correlation was obtained between the calculated electronic potentials of N(1) and N(3) nitrogen atoms and the experimental pK_a values for the ground and excited state deprotonation. Recent theoretical studies using the DFT approach have confirmed the role of the hydrogen-bonded complexes, yielding several stable eight-membered cyclic structures of lumichrome/acetic acid complexes characterized by spectral changes similar to those observed experimentally.[30] Spectral and photophysical properties of lumichrome in a number of different protic and aprotic and polar and nonpolar solvents have been examined recently.[44] Time-dependent density-functional theory has been successfully applied to a number of iso- and alloxazines to predict ground state and triplet−triplet electronic absorption spectra with good correspondence to the measured transitions.[30,31,44−49]

The present paper describes a steady-state and time-resolved study on the ESDPT reaction in lumichrome and its 1- and 3-methyl and 1,3-dimethyl derivatives in ethanolic solutions. We also report quantum mechanical calculations that shed new light on the mechanism of the ESDPT reaction in the lumichrome/carboxylic acid systems. The present theoretical investigation aims at providing a more systematic insight into the problem of the concerted vs the stepwise mechanism. The structures and abbreviations of the lumichromes discussed here are presented in Figure 1.

Experimental Section

Materials. Lumichrome, ethanol, and acetic acid from Aldrich were used as received. The 1-methyl-, 3-methyl-, and 1,3-dimethyllumichrome derivatives were available from previous work.

Spectral and Photophysical Measurements. Fluorescence decays were measured using excitation at 380 nm and single photon timing technique on a fluorescence lifetime spectrophotometer, which has been described in detail elsewhere.[50] Briefly, on the excitation side, a Spectra-Physics picosecond/femtosecond laser system is used as the source of exciting pulses. A Tsunami Ti:sapphire laser, pumped with a BeamLok 2060 argon ion laser, tunable in the 720−1000 nm range, generates 1−2 ps pulses at a repetition rate of about 82 MHz, and mean power of over 1 W. A model 3980-2S pulse selector reduces the repetition rate to the range from 4 MHz to single shot. Second and third harmonics of the picosecond pulse obtained on a GWU-23PS harmonic generator may be used for excitation. Elements of an Edinburgh Instruments FL900 system were used in the optical and control units of the system. The pulse timing and data processing systems employ a biased TAC model TC 864 (Tenelec) and the R3809U-05 MCP−PMT emission detector with thermoelectric cooling and appropriate preamplifiers (Hamamatsu). Steady-state fluorescence spectra were obtained with a Jobin Yvon-Spex Fluorolog 3−11 spectrofluorometer, and UV−visible absorption spectra on a Varian Cary 5E spectrophotometer. Unless otherwise indicated, the samples were in equilibrium with air. All measurements were performed at room temperature.

Laser-Induced Fluorescence (LIF) emission measurements of the samples were performed at room temperature in the front-face arrangement. The detailed description together with a diagram of the system had been presented in reference.[51] In brief, the system uses the 337.1 nm pulse (suitable for lumichrome excitation) of a N_2 laser (Photon Technology Instruments, model 2000, ca. 600 ps FWHM, ∼1.3 mJ/pulse) as the excitation source. The light arising from the irradiation of samples by the laser pulse is collected by a collimating beam probe coupled to an optical fiber (fused silica) and detected by a gated intensified charge coupled device (ICCD, Oriel model Instaspec V). The ICCD is coupled to a fixed compact imaging spectrograph (Oriel, model FICS 77441). The system can be used either by capturing all light emitted by the sample or in the time-resolved mode by using a delay generator (Stanford Research Systems, model DG535) with a suitable gate width. The ICCD has high speed (2.2 ns) gating electronics and covers the 200−900 nm wavelength range. Time-resolved absorption and emission spectra are available in the nanosecond to second time range.[51−53]

Quantum Mechanical Calculations. Information on the electronic structure and geometry of lumichromes was obtained with the use of quantum-chemical density-functional theory (DFT) calculations. The calculations were performed using the B3LYP functional[54] in conjunction with a split-valence polarized basis set 6-31G($d^{\dagger}$,$p^{\dagger}$).[55] Full optimization of the geometrical

TABLE 1: Spectral and Photophysical Data for the Singlet States of Lumichromes in Ethanol[a]

compound	$\lambda_{max}{}^2$/nm	$\lambda_{max}{}^1$/nm	ϕ_F	λ_F/nm	τ_F/ps	$k_r/10^8\ s^{-1}$	$\Sigma k_{nr}/10^8\ s^{-1}$
lumichrome	339	384 (7700)	0.032	453	797	0.40	12
1-methyllumichrome	340	385 (7500)	0.033	453	878	0.38	11
3-methyllumichrome	340	383 (8000)	0.032	460	828	0.39	12
1,3-dimethyllumichrome	340	386 (7500)	0.031	461	868	0.36	11

[a] The positions of the two long-wavelength bands in the absorption spectra $\lambda_{max}{}^1$, $\lambda_{max}{}^2$ are given with the molar absorption coefficients in parentheses. The fluorescence quantum yield is ϕ_F, the lifetime of fluorescence is τ_F, the radiative rate constant is k_r, and the sum of nonradiative rate constants is Σk_{nr}.

parameters of the complex of the two reacting molecules at this level of theory produced two ground-state potential energy minima. A transition state connecting these minima was also found, and IRC (intrinsic reaction coordinate) calculations followed by full geometry optimization (pseudo-IRC) verified that the obtained transition state indeed connects these two energy minima. The vertical excitation energies and oscillator strengths were computed using time dependent (TD) approach as implemented in the Gaussian 03 program.[56] Predicted lowest-energy singlet−singlet transitions of lumichromes, $S_0 \rightarrow S_i$, were calculated for the ground-state geometry. The excitation energies computed using TD-B3LYP/6-31G(d†,p†) level of theory are estimated to be accurate within 2000−3000 cm^{-1}, usually requiring a shift toward the red to reproduce experimental spectra. However, regarding the quality of our spectral predictions it should be noted that the difference in the experimental transition energies in 1,4-dioxane solution between lumiflavin and lumichrome (22.7×10^3 and 26.4×10^3 cm^{-1}) is reproduced in the calculations (24.5×10^3 and 27.8×10^3 cm^{-1}) to within 0.5×10^3 cm^{-1},[44] with the predicted values blue-shifted as compared to the experimental ones by less than 2.0×10^3 cm^{-1}.

To gain insight into geometry relaxation of the first excited state, calculations at TD-B3LYP/6−31(d†,p†)//CIS/6-31G(d†,p†) level were carried out. A transition state was located for the first excited state during geometry optimization with CIS method (configuration interaction with single excitations), whose geometry closely resembled the S_0 transition state. However, all attempts to obtain transition state geometries for higher excitations failed. As the excited energy levels are close to each other and even change their order in the course of the reaction, it only took a couple of geometry optimization steps to find that the desired excited level got swapped with some other excited state. To overcome this difficulty and gain insight into the potential energy hypersurfaces of higher excited states, we performed a scan of single point calculations with TD-B3LYP method for geometries along the first excited-state reaction path for the first six singlet−singlet excitations. A similar, yet even simpler approach using CIS method to obtain the energy values for the excited state with geometries along ground-state reaction path employed by Chou et al.[57] has been proven to provide useful results in line with experimental findings.

Results and Discussion

Spectroscopic and Photophysical Properties. Spectroscopic properties of lumichrome, its 1- and 3-methyl, and 1,3-dimethyl derivatives, and other alloxazines in different solvents have been the subject of a number of previous studies.[26,31,41,44,45,48,58] The absorption spectrum of lumichrome in ethanol exhibits two absorption bands in the long wavelength region. The absorption spectra of lumichrome and its derivatives are essentially identical in the long wavelength region, as also happens in some other solvents examined earlier. The absorption and the corrected fluorescence excitation spectra agree well with each other for all the lumichrome derivatives studied. The molar absorption coefficients and the band positions of the lowest energy transitions for the four lumichromes examined in ethanol are listed in Table 1. The two strong long-wavelength absorption bands of these compounds, with their maxima in ethanol at about 336 and 385 nm, have been assigned to two independent π,π^* transitions.[26,39] In conformity, our recent theoretical studies predict that the transitions observed in all these lumichromes are of the π,π^* character. The two calculated lowest-energy π,π^* transitions are located at approximately 316 nm (31.7×10^3 cm^{-1}) and 359 nm (27.8×10^3 cm^{-1}), and are accompanied by two closely located n,π^* transitions at 313 nm (31.9×10^3 cm^{-1}) and 362 nm (27.6×10^3 cm^{-1}) of low oscillator strengths. Hence, the lowest-energy state is of the n,π^* character. The weak fluorescence emission of alloxazines, relative to isoalloxazines, results from the close spacing between the n,π^* and π,π^* excited singlet states, with the lowest-energy state being of n,π^* character.

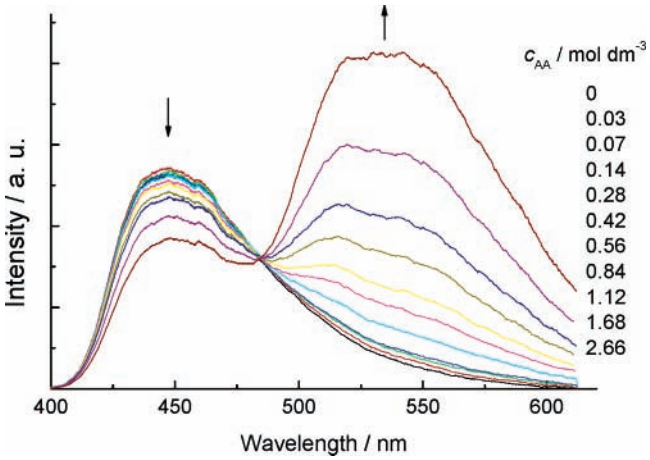

Figure 2. Effect of increasing acetic acid concentration on fluorescence emission spectra of lumichromes.

Changes in the absorption spectra are observed in the presence of the acetic acid, with an increase of acetic acid concentration for the two low-energy bands. We have discussed these changes in absorption of lumichrome and its derivatives in recent papers,[30,31,44] where 1,1,1,3,3,3-hexafluoroisopropanol was used as a hydrogen donor and DMSO as a hydrogen acceptor. The previous results allowed us to ascribe the changes in the absorption spectra of lumichromes mainly to the creation of hydrogen bonds in which the N(1) and N(10) nitrogen atoms are involved.

The fluorescence emission spectra of lumichrome and its derivatives in ethanol show a single band with the maximum at about 448 nm, the exact position of which depends on the location and number of substituents. Interestingly, a new long wavelength emission band appears for lumichrome, and 3-methyllumichrome in the presence of acetic acid; see Figure 2. The new emission with a maximum at about 527 nm is similar to the emission spectrum of the compounds with isoalloxazinic

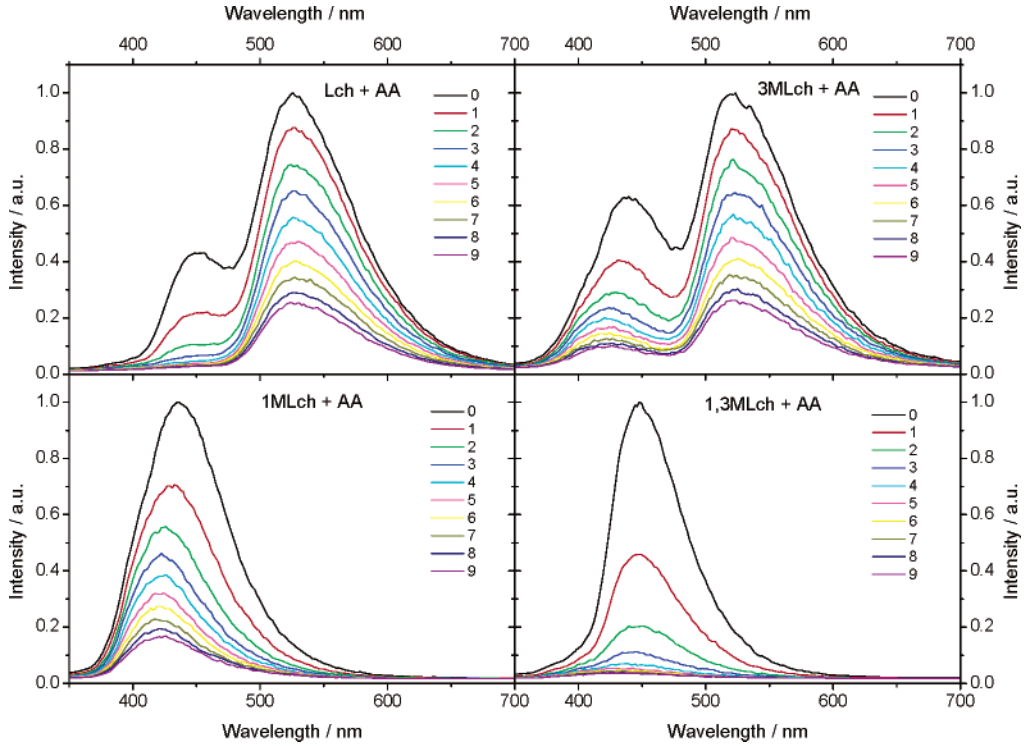

Figure 3. Time-resolved fluorescence spectra of lumichrome, 1-methyllumichrome, 3-methyllumichrome, and 1,3-dimethyllumichrome in ethanol with 2.79 mol dm^{-3} of acetic acid. Excitation was at 337 nm in all samples, the spectra were recorded with the time step of 1 ns.

structure (e.g., lumiflavin, riboflavin), and it has been identified as emission of the isoalloxazinic form appearing as a result of excited-state proton transfer from N(1) to N(10). The intensity of alloxazinic emission at about 446 nm decreased and the intensity of isoalloxazinic emission at about 527 nm increased with increasing acetic acid concentration. To help establish the role of N(1)−H and N(3)−H groups in proton transfer reaction, model compounds 1-methyllumichrome and 1,3-dimethyllumichrome were employed. The methyl group at N(1) and/or N(3) allows the effect of lumichrome−acetic acid interaction to be selectively observed. For N(1) substituted lumichromes, namely 1-methyllumichrome and 1,3-dimethyllumichrome, only alloxazinic emission is observed, whose intensity decreases with increasing acetic acid concentration.

We have performed time-resolved emission measurements in the nanosecond time range for lumichromes with (shown in Figure 3) and without (data not shown) acetic acid. The spectra without acetic acid obtained by the time-resolved method are almost identical for all samples and indicate single fluorescence maximum at about 445 nm, and in general, they closely reproduce the steady-state fluorescence spectra. The time evolution of the fluorescence spectra suggests that the fluorescence lifetimes are virtually constant throughout the spectrum, remaining in the nanosecond time range.

The time-resolved fluorescence emission spectra of lumichromes in ethanol in the presence of acetic acid (2.79 mol dm^{-3} AA), excited at 337 nm, are presented in Figure 3. As noted in the time-resolved fluorescence emission spectra, the isoalloxazinic band at longer wavelengths has a much longer fluorescence lifetime if compared to alloxazinic emission at shorter wavelengths. Similar to steady state fluorescence measurements, the new isoalloxazinic emission is only present for lumichrome and 3-methyllumichrome. On the other hand, for 1-methyllumichrome and 1,3-dimethyllumichrome, the time evolution of the fluorescence spectra indicate that only alloxazinic emission is present, with the fluorescence lifetime remaining largely unaffected by the presence of acetic acid.

To learn more about the kinetics of the excited-state process we employed the single photon timing technique to measure the emission lifetimes quantitatively. The decays of the emission of lumichrome in the presence and absence of acetic acid were measured in ethanol. The decays were monitored at the alloxazinic (450 nm) and isoalloxazinic (at 537 and 610 nm) emission bands. The typical decay curves are shown in Figure 4. The usage of these wavelengths allowed having better spectral resolution of the two types of emission, which was problematic in our earlier studies where photon counting systems with insufficient spectral and time resolution had been employed.[31,42]

The emission decay of lumichrome in ethanol is well described by a single exponential function. As shown in Table 2, the decay of alloxazinic emission at 450 nm of lumichrome with and without acetic acid is single-exponential in the whole range of acetic acid concentrations studied. The decay of the isoalloxazinic emission of lumichrome in the presence of acetic acid is described by a two-exponential function. For low acetic acid concentrations the function is a sum of two exponential decays, while for high acetic acid concentrations it is a sum of a single-exponential rise and a single-exponential decay. In both iso- and alloxazinic components, the fluorescence decay times become slightly shorter at higher acetic acid concentrations. Higher acetic acid concentrations also correspond to stronger contribution of the longer-lived decay component. The decay times of the alloxazinic emission are very close to the rise times of the isoalloxazinic emission for a given acetic acid concentration. These results allow a conclusion that in the excited state of lumichrome in the presence of acetic acid there is a kinetic relationship between the two excited forms; namely, the excited alloxazinic form is the precursor of the excited isoalloxazinic form. Moreover, the single-exponential decay of the alloxazinic form in the presence of acetic acid suggests that there is no

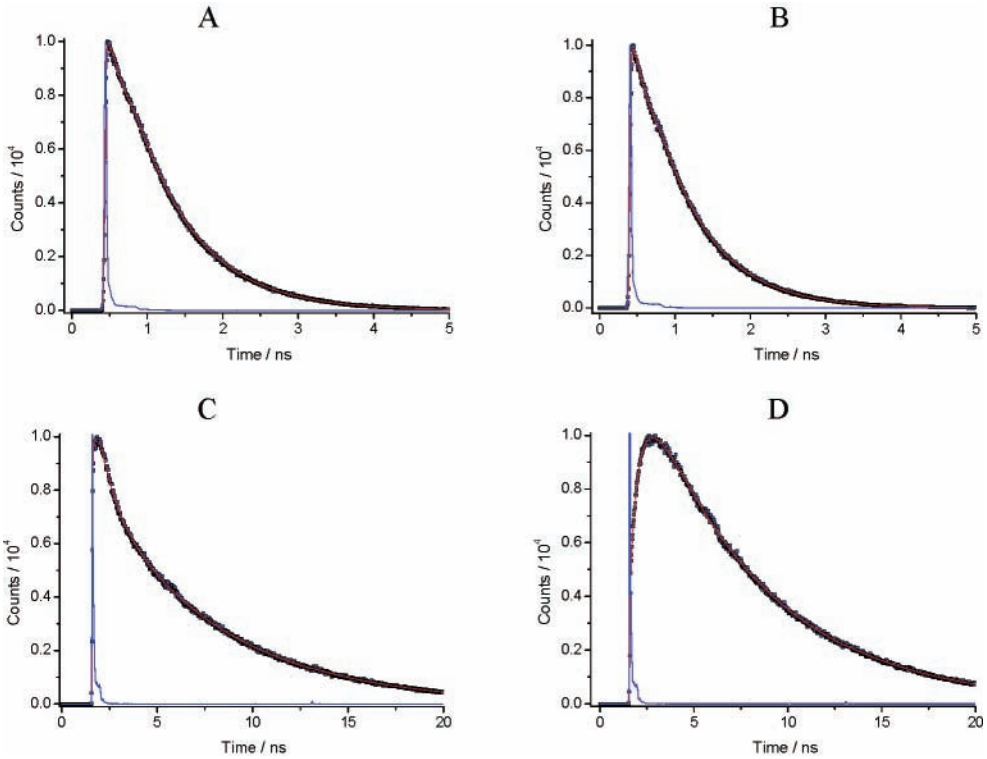

Figure 4. Typical fluorescence decays of lumichrome in ethanol. Panel A: without acetic acid, observed at 450 nm and fitted with a single-exponential function $\tau_F = 0.797$ ns, $\chi^2 = 1.002$, OR $= -1.191$, DW $= 1.872$. Panel B: with 1.53 mol dm^{-3} acetic acid and observed at 450 nm. Panel C: with 1.53 mol dm^{-3} acetic acid and observed at 537 nm. Panel D: with 1.53 mol dm^{-3} acetic acid and observed at 610 nm, see Table 2 for the curve fitting results.

TABLE 2: Fluorescence Lifetimes for Alloxazinic and Isoalloxazinic Forms of Lumichrome Measured at Various Acetic Acid Concentrations in Ethanol[a]

acetic acid concentration/mol dm^{-3}	450 nm		537 nm			610 nm		
	τ_F/ns	χ^2	τ_F^1/ns (a^1)	τ_F^2/ns (a^2)	χ^2	τ_F^1/ns (a^1)	τ_F^2/ns (a^2)	χ^2
	0.797	1.002						
0.275	0.777	1.079	0.801 (0.101)	6.476 (0.018)	1.025	0.844 (0.050)	6.454 (0.060)	1.117
0.54	0.760	1.027	0.790 (0.080)	6.448 (0.031)	1.129	0.800 (0.032)	6.433 (0.9681)	1.186
1.53	0.698	1.176	0.786 (0.030)	6.276 (0.071)	1.153	0.646 (−0.885)	6.270 (1.885)	1.136
2.30	0.637	1.184	0.786 (0.113)	6.109 (0.887)	1.181	0.614 (−1.127)	6.108 (2.127)	1.163

[a] See the text for the discussion.

equilibrium between both tautomeric forms in the excited state. According to these conclusions, the data in Table 2 were analyzed using a simple kinetic model. In the model the alloxazinic component deactivates to the ground state with a k_A rate constant and forms the isoalloxazinic component with a k_{AB} rate constant multiplied by the acetic acid concentration. The isoalloxazinic component decays to the ground state with a k_B rate constant, while it re-forms the alloxazinic component with a k_{BA} rate constant. The four rate constants were determined using the method described by Laws and Brand.[59] The k_{BA} rate constant was found to have very low values, while the other rate constant values were determined as follows: $k_A = 1.25 \times 10^9$ s^{-1}, $k_B = 1.9 \times 10^8$ s^{-1}, and $k_{AB} = 1.4 \times 10^8$ dm^3 mol^{-1} s^{-1}.

Ground-State Proton Transfer. DFT calculations identified two potential energy minima in the ground state, corresponding to the tautomeric forms **a** and **b** of lumichrome interacting with carboxylic acid (see Figure 5). The lowest energy structure corresponds to form **a**, while the tautomeric form **b** is higher in energy by about 6 kcal/mol at the B3LYP level of theory. These two potential energy minima are connected via a transition state ($\mathbf{TS}_{ground}$), with the relative energy of ca. 9.4 kcal/mol. Thus, the activation barrier for the reaction converting tautomer **a** into **b** is ca. 9.4 kcal/mol, while that for the reverse reaction

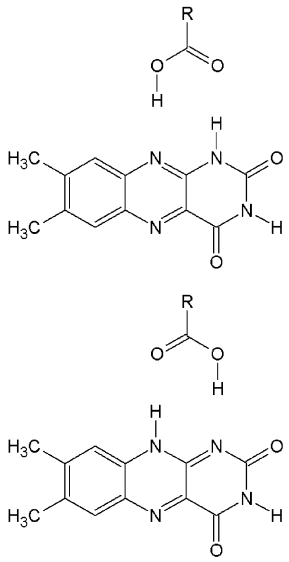

Figure 5. Tautomeric forms: (**a**) top; (**b**) bottom.

is ca. 3.2 kcal/mol; see Figure 6. Table 3 presents selected geometrical parameters describing the complex of lumichrome with carboxylic acid in its ground state. The bond lengths in

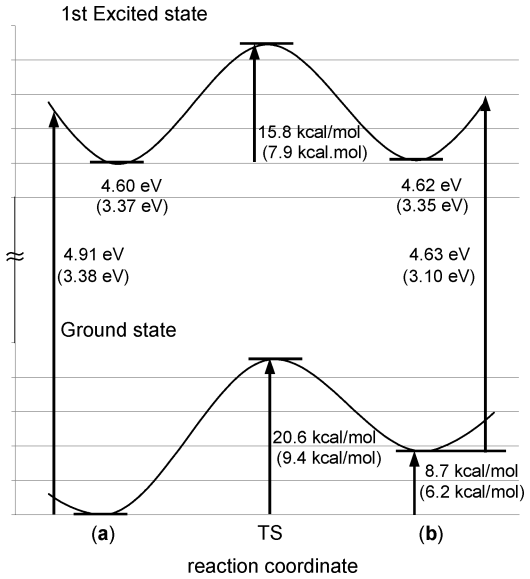

Figure 6. Energies of the tautomers **a** and **b** and of the transition states (TS) connecting them, calculated for the ground state and the first singlet−singlet excited state of lumichrome, at the CIS/6-31G($d^{\dagger}$,$p^{\dagger}$) level. Values shown in parentheses were obtained at the B3LYP/6-31G($d^{\dagger}$,$p^{\dagger}$) level for the ground state and TD-B3LYP/6-31($d^{\dagger}$,$p^{\dagger}$)//CIS/6-31G($d^{\dagger}$,$p^{\dagger}$) level for the first excited state.

TABLE 3: Relative Energies and Selected Geometrical Parameters of the a, b, and TS_{ground} Structures of the Lumichrome−Formic Acid Complex

	a	**b**	$\mathbf{TS_{ground}}$
ΔE [kcal/mol][a]	0.0	6.2	9.4
N(1)−H [Å]	1.031	1.685	1.237
(N(1))H···O(acid) [Å]	1.843	1.022	1.268
N(1)···O(acid) [Å]	2.866	2.707	2.505
∠N(1)HO [deg]	171.0	179.3	179.8
O−H(acid) [Å]	1.010	1.705	1.456
(O)H···N(10) [Å]	1.729	1.044	1.110
O···N(10) [Å]	2.736	2.748	2.566
∠OHN(10) [deg]	174.7	176.4	179.5

[a] Calculated at B3LPY/6-31G($d^{\dagger}$,$p^{\dagger}$) level. The absolute energy level is −1022.629348 hartree.

the transition state are 1.237 and 1.268 Å, for the N(1)···H and (N(1))H···O(acid) distances, respectively. The same distances in tautomer **a** are 1.031 and 1.843 Å, while in structure **b** they are 1.685 and 1.022 Å. These values indicate that the hydrogen atom gets transferred between the N(1) atom of lumichrome and the O atom of carboxylic acid in the proton exchange reaction. Regarding the N(10)···H and O···H(acid) distances corresponding to proton acceptor hydrogen bonds in structure **a**, their values in the transition state are 1.110 and 1.456 Å, respectively. The same distances are 1.729 and 1.010 Å in the **a** structure, while 1.044 and 1.705 Å in the **b** structure. Thus, the transition state geometry is in fact closer to the **b** tautomer than to the **a** one, as we would expect from the respective energies. The geometry changes corresponding to the imaginary frequency in the transition state are presented in the Supporting Information to this paper as an animation. Interestingly, the obtained values seem to indicate that the proton transfer from the O atom of carboxylic acid to the N(10) atom of lumichrome immediately triggers such changes within the complex that the transfer of the other proton from N(1) of lumichrome to carboxylic acid is barrierless in terms of energy. Thus, the exchange of both protons seems to occur in a concerted asynchronous way, as IRC calculations indicate that the

TABLE 4: Vertical Excitation Energies E (cm^{-1}) Calculated at TD-B3LYP and CIS Levels for the a and b Tautomers

	E/cm^{-1}	
	a	**b**
n,π^* (B3LYP)	27 584	25 568
n,π^* (CIS)	40 005	38 473
π,π^* (B3LYP)	27 262	25 003
π,π^* (CIS)	39 602	37 343

($\mathbf{TS_{ground}}$) transition state indeed connects the tautomeric structures **a** and **b**.

Excitation Energies. Vertical excitation energies calculated at TD-DFT and CIS levels of theory are presented in Table 4. The geometries of the **a** and **b** tautomers optimized at the B3LYP level of theory were utilized in the TD-DFT calculations, while the same geometries optimized at the HF level of theory were used in the CIS calculations. In line with earlier findings of Chou et al. for 3-formyl-7-azaindole,[57] the calculated CIS values of the excitation energies are significantly higher than those obtained from the time-dependent DFT calculations. The lowest excited singlet state is predicted to be π,π^* with a closely lying n,π^* state, for tautomeric form **a** of the lumichrome−carboxylic acid complex. Same as many of the aza-aromatics, lumichrome and its complexes with carboxylic acid possess close-neighboring n,π^* and π,π^* singlet excited states,[30] with the calculated $\Delta E = 0.3 \times 10^3$ cm^{-1} for tautomer **a**. The second π,π^* transition is also accompanied by a closely lying n,π^* transition. The respective vertical excitation energies as obtained from the time-dependent DFT calculations for tautomer **a** are as follows: 27.3×10^3 cm^{-1} for the first π,π^* excitation, essentially from HOMO to LUMO, 31.1×10^3 cm^{-1} for the second π,π^* excitation, essentially from HOMO-1 to LUMO; 27.6×10^3 cm^{-1} for the first n,π^* excitation, mainly from HOMO-2 to LUMO; and 30.9×10^3 cm^{-1} for the second n,π^* excitation, chiefly from HOMO-3 to LUMO (see Figure 7).

The vertical excitation energy of 25.0×10^3 cm^{-1} for the **b** tautomer corresponds to the π,π^* excitation, chiefly from HOMO to LUMO, while the value of 25.6×10^3 cm^{-1} corresponds to the n,π^* excitation, mainly from HOMO-1 to LUMO. While the TD-B3LYP and CIS calculations for the **a** tautomer produced the same predominant molecular orbitals involved in the n,π^* and π,π^* excitations, the CIS calculations for the **b** tautomer indicate that HOMO-4 and LUMO orbitals are involved in the n,π^* excitation. However, the character of HOMO-4 obtained from CIS calculations is very similar to that of HOMO-1 obtained from TD-B3LYP calculations, whereas the energy order of the orbitals is different in the two approaches.

Excited-State Proton Transfer. As mentioned earlier, the calculations leading to transition states connecting "normal" (**a**) and "tautomeric" (**b**) forms of lumichrome in its complex with carboxylic acid were successful only for the first excited state. For higher transition states, the desired excitation level was substituted by another, lower-energy one, after just a couple of geometry optimization steps. The rationale seems to be the very small energy differences between excited states and the change in their order in the course of the reaction (see Figure 8). The fourth excited state of the **a** tautomeric form correlates to the second excited state in the **b** form. Table 5 presents the estimates of relative energies at TD-B3LYP/6-31G($d^{\dagger}$,$p^{\dagger}$) level for geometries along the reaction path in the first excited-state calculated at CIS/6-31G($d^{\dagger}$,$p^{\dagger}$) level for the **a** and **b** tautomeric forms as well as for the transition barrier interconnecting them.

The activation barrier for the reaction converting **a** into **b** estimated at various excited states is in the range from 0.0 to

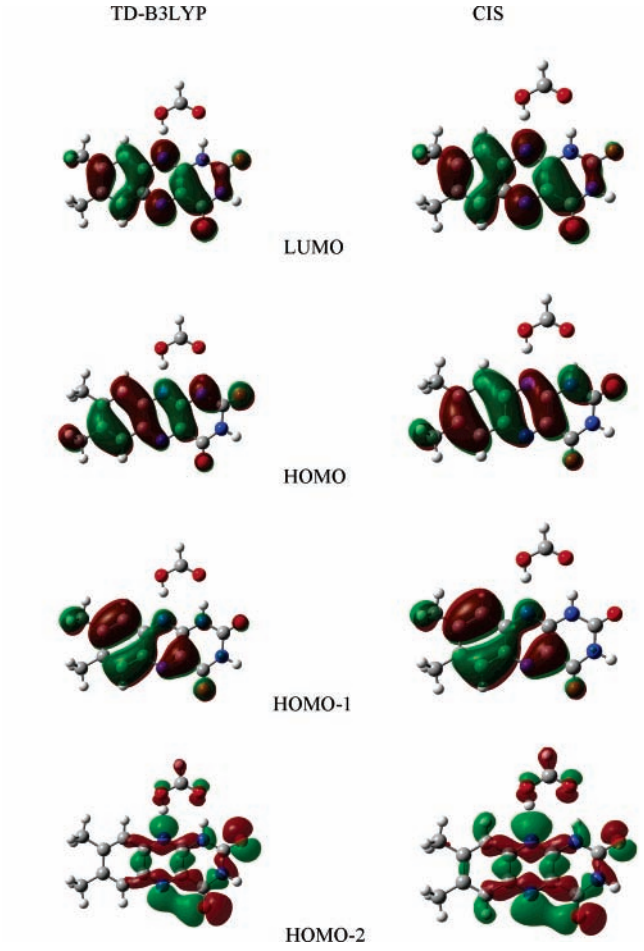

Figure 7. Molecular orbitals calculated for the (**a**) tautomer of lumichrome interacting with formic acid. The n → π^* excitation chiefly involves HOMO-2 and LUMO (second excitation) and HOMO-3 and LUMO (third excitation), calculated at both TD-B3LYP and CIS levels, while $\pi \rightarrow \pi^*$ excitation mainly involves HOMO and LUMO (first excitation) and HOMO-1 and LUMO (fourth excitation) as calculated at TD-B3LYP and CIS levels.

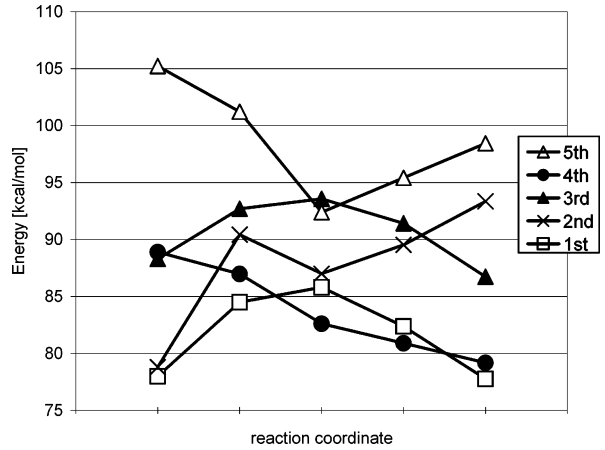

Figure 8. Potential energy hypersurface for the first six singlet−singlet excited states. Note that the fourth excited state of the **a** tautomer in the course of the reaction becomes the second excited state of the **b** tautomer.

over 14 kcal/mol. The results obtained indicate that the activation barrier for the reaction leading from tautomer **a** to **b** does not exist in the fourth excited state and that the respective conversion is barrierless. Interestingly, for carboxylic acid-catalyzed proton transfer in 3-formyl-7-azaindole, the reaction proceeded toward the tautomeric form of azaindole without any energy barrier in the second singlet−singlet excited state.[57] In the present case of lumichrome in complex with a carboxylic acid, the theory applied favors the reaction in the excited state, indicating the absence of any stable intermediate state. These results follow from the evolution of the potential energy hypersurfaces for the ground and the first singlet excited state in the course of the ground-state reaction, supporting at least theoretically the concerted asynchronous mechanism of the ESDPT reaction in the lumichrome−formic acid system. Similar to the ground-state reaction, the exchange of both protons in the first excited state seems to occur in a concerted way, as our pseudo-IRC calculations indicate that the transition state indeed connects the tautomeric structures **a** and **b** in the first excited state.

TABLE 5: Relative Energies Calculated at TD-B3LYP/6-31G(d†,p†)//CIS/6-31G(d†,p†) Level for the First Five Singlet−Singlet Excited States and the Ground State[a]

	a	activation barrier	**b**
ground state	0.0	9.4	6.2
1st excited state	0.0	7.8	−0.2
2nd excited state	0.0		14.5[b]
3rd excited state	0.0	5.3	−1.6
4th excited state	0.0[a]		−9.7
5th excited state	0.0		−6.8[b,c]

[a] Energies of the **b** tautomer and the activation barrier for the reaction converting **a** into **b** are shown in kcal/mol as values relative to those of the **a** tautomer. [b] An unstable structure. [c] The energy minimum corresponds to the protonated lumichrome cation and carboxylic anion.

Conclusions

The activation energy barrier present for carboxylic acid-catalyzed double proton transfer in the ground state is significantly lower in the first excited state, vanishing in the fourth excited state of the lumichrome−acid hydrogen-bonded complex. The activation barrier for the reaction is estimated to be about 9.5 kcal/mol (B3LYP) in the ground state, about 7.8 kcal/mol in the first excited state, while in the fourth excited state tautomer **a** undergoes a barrierless transition leading to tautomer **b**.

Acknowledgment. The authors thank a reviewer for the suggestion on using the term "asynchronous concerted double proton transfer". Interdisciplinary Grant No. 51103-504 from the A. Mickiewicz University and the University of Economics, Poznań, Poland, to M.S. and E.S., is gratefully acknowledged. All of the calculations were performed at the Poznań Supercomputing and Networking Centre (PCSS). The fluorescence lifetime measurements were performed at the Center for Ultrafast Laser Spectroscopy, Adam Mickiewicz University, Poznań, Poland.

Supporting Information Available: An animation (.avi) presenting the geometry changes corresponding to the imaginary frequency in the transition state of lumichrome-formic acid system indicating the exchange of both protons in a concerted asynchronous way. This material is available free of charge via the Internet at http://pubs.acs.org.

References and Notes

(1) Taylor, C. A.; El-Bayoumi, M. A.; Kasha, M. *Proc. Natl. Acad. Sci. U.S.A.* **1969**, *63*, 253.
(2) Takeuchi, S.; Tahara, T. *Chem. Phys. Lett.* **2001**, *347*, 108.
(3) Takeuchi, S.; Tahara, T. *J. Phys. Chem. A* **1998**, *102*, 7740.
(4) Douhal, A.; Moreno, M.; Lluch, J. M. *Chem. Phys. Lett.* **2000**, *324*, 81.

(5) Fiebig, T.; Chachisvilis, M.; Manger, M.; Zewail, A. H.; Douhal, A.; Garcia-Ochoa, I.; de La Hoz Ayuso, A. *J. Phys. Chem. A* **1999**, *103*, 7419.

(6) Chachisvilis, M.; Fiebig, T.; Douhal, A.; Zewail, A. H. *J. Phys. Chem. A* **1998**, *102*, 669.

(7) Catalan, J.; Kasha, M. *J. Phys. Chem. A* **2000**, *104*, 10812.

(8) Douhal, A.; Guallar, V.; Moreno, M.; Lluch, J. M. *Chem. Phys. Lett.* **1996**, *256*, 370.

(9) Catalan, J.; Perez, P.; Del Valle, J. C.; De Paz, J. L. G.; Kasha, M. *Proc. Natl. Acad. Sci. U.S.A.* **2002**, *99*, 5793.

(10) Catalan, J.; Perez, P.; Del Valle, J. C.; De Paz, J. L. G.; Kasha, M. *Proc. Natl. Acad. Sci. U.S.A.* **2002**, *99*, 5799.

(11) Catalan, J.; Del Valle, J. C.; Kasha, M. *Proc. Natl. Acad. Sci. U.S.A.* **1999**, *96*, 8338.

(12) Douhal, A.; Moreno, M.; Lluch, J. M. *Chem. Phys. Lett.* **2000**, *324*, 75.

(13) Catalan, J.; Del Valle, J. C.; Kasha, M. *Chem. Phys. Lett.* **2000**, *318*, 629.

(14) Waluk, J. *Conformational Analysis of Molecules in Excited States*; Wiley-VCH: New York, 2000.

(15) Agmon, N. *J. Phys. Chem. A* **2005**, *109*, 13.

(16) Sakota, K.; Sekiya, H. *J. Phys. Chem. A* **2005**, *109*, 2718.

(17) Sakota, K.; Sekiya, H. *J. Phys. Chem. A* **2005**, *109*, 2722.

(18) Sakota, K.; Okabe, C.; Nishi, N.; Sekiya, H. *J. Phys. Chem. A* **2005**, *109*, 5245.

(19) Hara, A.; Sakota, K.; Nakagaki, M.; Sekiya, H. *Chem. Phys. Lett.* **2005**, *407*, 30.

(20) Komoto, Y.; Sakota, K.; Sekiya, H. *Chem. Phys. Lett.* **2005**, *406*, 15.

(21) Hara, A.; Komoto, Y.; Sakota, K.; Miyoshi, R.; Inokuchi, Y.; Ohashi, K.; Kubo, K.; Yamamoto, E.; Mori, A.; Nishi, N.; Sekiya, H. *J. Phys. Chem. A* **2004**, *108*, 10789.

(22) Sakota, K.; Hara, A.; Sekiya, H. *Phys. Chem. Chem. Phys.* **2004**, *6*, 32.

(23) Kozioł, J. *Experientia* **1965**, *21*, 189.

(24) Kozioł, J. *Photochem. Photobiol.* **1966**, *5*, 41.

(25) Song, P. S.; Sun, M.; Koziołowa, A.; Kozioł, J. *J. Am. Chem. Soc.* **1974**, *96*, 4319.

(26) Koziołowa, A. *Photochem. Photobiol.* **1979**, *29*, 459.

(27) Koziołowa, A.; Visser, A. J. W. G.; Kozioł, J. *Photochem. Photobiol.* **1988**, *48*, 7.

(28) Kasha, M. *J. Chem. Soc., Faraday Trans. 2* **1986**, *82*, 2379.

(29) Chou, P. T.; Wei, C. Y.; Chang, C. P.; Chiu, C. H. *J. Am. Chem. Soc.* **1995**, *117*, 7259.

(30) Sikorska, E.; Khmelinskii, I. V.; Kubicki, M.; Prukała, W.; Nowacka, G.; Siemiarczuk, A.; Koput, J.; Ferreira, L. F. V.; Sikorski, M. *J. Phys. Chem. A* **2005**, *109*, 1785.

(31) Sikorska, E.; Koziołowa, A.; Sikorski, M.; Siemiarczuk, A. *J. Photochem. Photobiol. A* **2003**, *157*, 5.

(32) Koziołowa, A.; Visser, N. V.; Kozioł, J.; Szafran, M. M. *J. Photochem. Photobiol. A* **1996**, *93*, 157.

(33) Zen, Y. H.; Wang, C. M. *J. Chem. Soc., Chem. Commun.* **1994**, 2625.

(34) Tyrakowska, B.; Koziołowa, A.; Bastiaens, P. I. H.; Visser, A. J. W. G. *Flavins and Flavoproteins 1990* **1991**, 45.

(35) MacInnis, J. M.; Kasha, M. *Chem. Phys. Lett.* **1988**, *151*, 375.

(36) Song, P. S.; Choi, J. D. *Bull. Korean Chem. Soc.* **1980**, *1*, 93.

(37) Choi, J. D.; Fugate, R. D.; Song, P. S. *J. Am. Chem. Soc.* **1980**, *102*, 5293.

(38) Fugate, R. D.; Song, P. S. *Photochem. Photobiol.* **1976**, *24*, 479.

(39) Sun, M.; Moore, T. A.; Song, P. S. *J. Am. Chem. Soc.* **1972**, *94*, 1730.

(40) Heelis, P. F.; Koziołowa, A. *J. Photochem. Photobiol. B* **1991**, *11*, 365.

(41) Sikorska, E.; Szymusiak, H.; Khmelinskii, I. V.; Koziołowa, A.; Spanget-Larsen, J.; Sikorski, M. *J. Photochem. Photobiol.* A **2003**, *158*, 45.

(42) Sikorska, E.; Koziołowa, A. *J. Photochem. Photobiol. A* **1996**, *95*, 215.

(43) Dzugan, T. P. A study of the proton transfer of 3-hydroxyflavone and lumichrome using picosecond time-resolved spectroscopy. Ph.D. Thesis, Florida State University, 1987.

(44) Sikorska, E.; Khmelinskii, I. V.; Prukała, W.; Williams, S. L.; Patel, M.; Worrall, D. R.; Bourdelande, J. L.; Koput, J.; Sikorski, M. *J. Phys. Chem. A* **2004**, *108*, 1501.

(45) Sikorska, E.; Khmelinskii, I. V.; Bourdelande, J. L.; Bednarek, A.; Williams, S. L.; Patel, M.; Worrall, D. R.; Koput, J.; Sikorski, M. *Chem. Phys.* **2004**, *301*, 95.

(46) Sikorska, E.; Khmelinskii, I. V.; Koput, J.; Sikorski, M. *J. Mol. Struct. (THEOCHEM)* **2004**, *676*, 155.

(47) Sikorska, E.; Khmelinskii, I. V.; Prukała, W.; Williams, S. L.; Worrall, D. R.; Bourdelande, J. L.; Bednarek, A.; Koput, J.; Sikorski, M. *J. Mol. Struct.* **2004**, *689*, 121.

(48) Sikorska, E.; Khmelinskii, I. V.; Williams, S. L.; Worrall, D. R.; Herance, R. J.; Bourdelande, J. L.; Koput, J.; Sikorski, M. *J. Mol. Struct.* **2004**, *697*, 199.

(49) Sikorska, E.; Khmelinskii, I. V.; Koput, J.; Bourdelande, J. L.; Sikorski, M. *J. Mol. Struct.* **2004**, *697*, 137.

(50) Karolczak, J.; Komar, D.; Kubicki, J.; Wróżowa, T.; Dobek, K.; Ciesielska, B.; Maciejewski, A. *Chem. Phys. Lett.* **2001**, *344*, 154.

(51) Botelho do Rego, A. M.; Ferreira, L. F. V. Photonic and Electronic Spectroscopies for the Characterization of Organic Surfaces and Organic Molecules Adsorbed on Surfaces. In *Handbook of Surfaces and Interfaces of Materials*; Nalwa, H. S., Ed.; Academic Press: New York, 2001; Vol. 2; Chapter 7.

(52) Ferreira, L. F. V.; Machado, I. F.; Da Silva, J. P.; Oliveira, A. S. *Photochem. Photobiol. Sci.* **2004**, *3*, 174.

(53) Ferreira, L. F. V.; Machado, I. F.; Oliveira, A. S.; Ferreira, M. R. V.; Da Silva, J. P.; Moreira, J. C. *J. Phys. Chem. B* **2002**, *106*, 12584.

(54) Becke, A. D. *J. Chem. Phys.* **1993**, *98*, 5648.

(55) Ditchfield, R.; Hehre, W. J.; Pople, J. A. *J. Chem. Phys.* **1971**, *54*, 724.

(56) Frisch, M. J.; Trucks, G. W.; Schlegel, H. B.; Scuseria, G. E.; Robb, M. A.; Cheeseman, J. R.; Zakrzewski, V. G.; Montgomery, A. J., Jr.; Stratmann, R. E.; Burant, J. C.; Dapprich, S.; Millam, J. M.; Daniels, A. D.; Kudin, K. N.; Strain, M. C.; Farkas, O.; Tomasi, J.; Barone, V.; Cossi, M.; Cammi, R.; Mennucci, B.; Pomelli, C.; Adamo, C.; Clifford, S.; Ochterski, J.; Petersson, G. A.; Ayala, P. Y.; Cui, Q.; Morokuma, K.; Malick, D. K.; Rabuck, A. D.; Raghavachari, K.; Foresman, J. B.; Cioslowski, J.; Ortiz, J. V.; Stefanov, B. B.; Liu, G.; Liashenko, A.; Piskorz, P.; Komaromi, I.; Gomperts, R.; Martin, R. L.; Fox, D. J.; Keith, T.; Al-Laham, M. A.; Peng, C. Y.; Nanayakkara, A.; Gonzalez, C.; Challacombe, M.; Gill, P. M. W.; Johnson, B.; Chen, W.; Wong, M. W.; Andres, J. L.; Gonzalez, C.; Head-Gordon, M.; Replogle, E. S.; Pople, J. A. Gaussian 98, Revision A.11.3.; Gaussian, Inc.: Pittsburgh, PA, 2002.

(57) Hung, F. T.; Hu, W. P.; Chou, P. T. *J. Phys. Chem. A* **2001**, *105*, 10475.

(58) Koziołowa, A.; Szymusiak, H.; Kozioł, J. *Pol. J. Chem.* **1993**, *67*, 1813.

(59) Laws, W. R.; Brand, L. *J. Phys. Chem.* **1979**, *83*, 795.